

Optical and electrical properties of holmium thin films as a function of hydrogen concentration

D.E. Azofeifa*, W.E. Vargas, N. Clark, H. Solís

Centro de Investigación en Ciencia e Ingeniería de Materiales, Escuela de Física, Universidad de Costa Rica, San José, Costa Rica

Received 30 September 2006; received in revised form 9 February 2007; accepted 13 February 2007

Available online 16 February 2007

Abstract

We measure the evolution of the optical transmission (200–760 nm) and the electrical resistivity of Ho films, 50 nm thick, as a function of H concentration up to 2.9 [H]/[Ho]. The Ho films are covered with a 15 nm thick Pd overcoat for hydrogenation and ex situ measurements. Concentration is measured using a quartz crystal microbalance; the films are deposited in a high vacuum chamber and all measurements are made at room temperature. From the measured transmission spectra, using an inversion method, the complex refraction index of the Ho film is determined; from it the dielectric function, $\varepsilon = \varepsilon_1 + i\varepsilon_2$, is calculated. This procedure is applied to the hydrogenated Pd coated Ho films finding the evolution of ε as a function of hydrogen concentration. Furthermore, using the inversion method in the trihydrided films the plasma frequency and the band gap are calculated.

© 2007 Elsevier B.V. All rights reserved.

Keywords: Hydrogen storage materials; Thin film; Electronic transport

1. Introduction

Hydrogen absorption in rare earths (RE) has been extensively studied in many and diverse forms. Of particular interest has been the study of their optical properties after the discovery by Huiberts et al. [1] of their dramatic changes upon reaching the trihydride phase. Although more complex systems [2,3] are now the center of study for possible application as switchable mirrors [4], their study continues trying to understand further aspects of the basic phenomena involved [5].

As one of the RE, holmium also shows the metal-insulator transition as it absorbs hydrogen and concentration nears 3 [6]. However, very few works centered on its optical properties are found in the literature and to our knowledge, none on Ho thin films. In this work we present the evolution of the transmission spectra of these films as hydrogen is absorbed and extract further information from them.

2. Experimental

2.1. Deposition and hydrogenation

The films are prepared in a high vacuum chamber at a 4×10^{-7} Torr base pressure by electron beam deposition. The Ho (3N) films are deposited on quartz substrates and immediately covered with a Pd (3N) protection layer to allow ex situ optical measurements. Their thicknesses are between 50 nm and 70 nm for the Ho films and between 12 nm and 17 nm for the Pd overcoat. Their geometric form is a 1.2 cm diameter circle which allows simultaneous measurements of transmission and resistivity. Further details of the sample preparation are given in [7]. A twin sample is deposited on a previously calibrated quartz crystal microbalance (QCM) to determine the concentration, $x = [\text{number of H atoms}]/[\text{number of metal atoms}]$, details are given in Ref. [8]. Once deposited, the bilayer is moved to a hydrogenation chamber which is evacuated to 2×10^{-5} Torr before hydrogen gas is allowed in. The pressure increase rate is around 20 mTorr/min up to 10 Torr. Thereafter the rate is increased to approximately 20 Torr/min until a maximum pressure of 600 Torr is reached. This slow rate is chosen to have the gas-film system in quasi-equilibrium and thus allowing concentration calculations using the QCM data. Due to the affinity of hydrogen with the RE, the hydrogen concentration in the as-deposited films, may not be exactly zero but within the uncertainty of our measurements the initial concentration is taken as such. Samples and measurements are made at room temperature.

2.2. Electrical and optical measurements

The electrical resistivity, ρ , is measured using the van der Pauw method [9] on the same sample on which the optical transmission is measured. The four

* Corresponding author. Tel.: +506 207 4705; fax: +506 225 5511.
E-mail address: deazofei@cariari.ucr.ac.cr (D.E. Azofeifa).

electrical contacts are placed at the end of two perpendicular diameters and the measurements are recorded by means of a data acquisition unit (Agilent 34970A). This unit also records the pressure measurement done with a baratron type meter.

The transmission spectra, $T_{\text{exp}}(\lambda)$, in the visible and near ultraviolet (200–750 nm) are taken with a spectrometer (Avantes 2048) illuminating from the Pd side with normally incident light. $T_{\text{exp}}(\lambda)$ is continuously measured as gas is slowly introduced in the hydrogenation chamber.

3. Results and discussion

3.1. From electrical measurements

The resistivity of the Ho film, ρ_{Ho} , is calculated assuming a parallel model in the bilayer and the known behavior as a function of H pressure for the resistivity of the Pd coating (ρ_{Pd}). As depicted in Fig. 1, $\rho_{\text{Ho}}(x)$ has a similar behavior to other RE's. After a small initial increase (maximum at $x=0.21$), it decreases reaching a minimum of $0.2\rho_{\text{Ho}}(0)$ as concentration nears 2.0, and then it shows a large increase which begins as concentration nears 2.1. This increase indicates that the trihydride is being formed and the M–I transition has occurred.

3.2. From optical measurements

The optical transmission measurements as a function of wavelength and hydrogen concentration for a bilayer are shown in Fig. 2. The large increase in $T_{\text{exp}}(\lambda)$ for concentrations larger than 2.2 indicates that the M–I took place in the Ho film. This increase is smaller for shorter wavelengths, i.e., higher energies, and disappears below 370 nm. Also, as in other RE:H systems, a transmission window occurs approximately centered on $x=2$. In the case of Ho this window is noticeable from $\lambda=370$ nm to the highest λ measured and for $1.9 < x < 2.1$.

From these measured spectra, $T_{\text{exp}}(\lambda, x)$, the values of refractive index and extinction coefficient of the Pd, n and k , and of the Ho, N and K , are retrieved. From them the complex dielec-

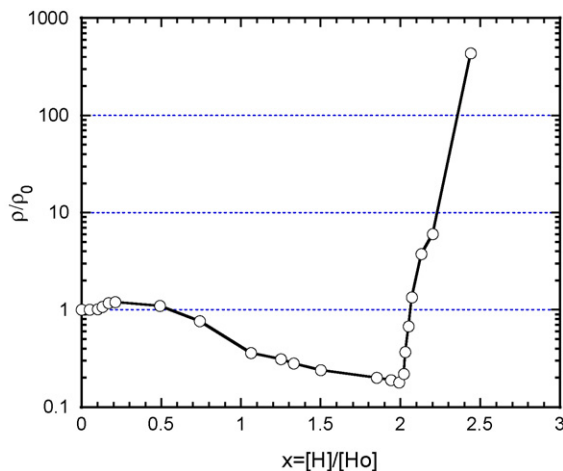


Fig. 1. Normalized resistivity of a Ho film 60.2 nm thick capped with 12.6 nm Pd film as a function of hydrogen concentration. The data was obtained assuming a parallel behavior in the bilayer. Initial resistivity for the Ho film is $\rho_0 = 121.5 \mu\Omega \text{ cm}$. A rapid increase occurs as H-concentration increases above 2 indicating a M–I transition.

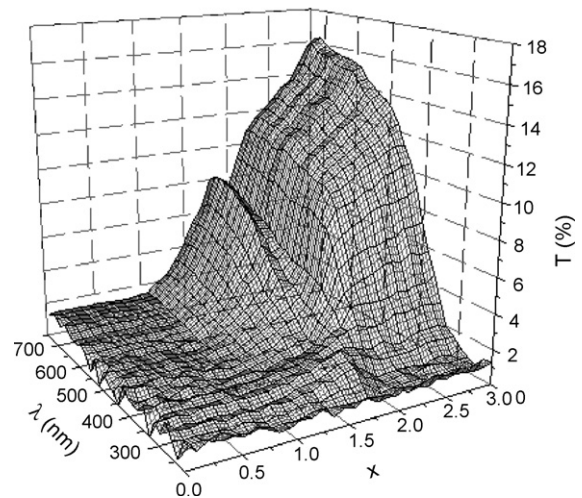


Fig. 2. Transmission of a Ho(50.1 nm)/Pd(12.6 nm) bilayer as a function of H concentration in the Ho film and wavelength. The large increase in the visible region indicates the M–I transition in the Ho film. The transmission window centered at $x \approx 2$ is clear in the region between 375 nm and 750 nm.

tric functions for each metal are calculated. In this form their evolution as a function of hydrogen concentration is studied. The retrieving procedure was done applying an optimization method based on a projected gradient formalism. The details of this numerical approach have been published elsewhere [10–12]. The optimization gradient methods require an initial estimation of the optical constants of the bilayer component materials. In the spectral region considered, the quartz substrate is taken as non-absorbing material, whose optical constants have been taken from the literature [13]. For the Pd coating layer values of n and k were taken from [14] (see circles in Fig. 3a) and used as a first approximation for the optical constants during all the optimization calculations. As for the initial values of N and K , the optical constants of Ho, we used those reported by Weaver and Lynch [15] made on crystalline Ho samples (see circles in Fig. 3b). The retrieved values of the dielectric function, $\varepsilon = \varepsilon_1 + i\varepsilon_2$, for both metals are shown in Fig. 3. As expected both materials display a metallic character in the visible and near ultraviolet, with negative values for ε_1 and decreasing ε_2 as energy increases. Additionally Ho results show some structure for energies around 2 eV and a departure from the crystalline sample behavior in the UV region. However, the close similarity between the retrieved values and those reported, indicates that contamination in our samples is not significant.

The optimized values for the Pd and Ho optical constants of the as-deposited unhydrided bilayer system were used as the first approximation for the optical constants of the hydrided Pd coated Ho film with $x=0.56$ to invert the corresponding transmittance spectrum. This new solution provides a first approximation of the optical constants of the hydrided Pd coated Ho film for the following concentration considered, and so on. The results are depicted in Fig. 4 where the spectral dependence of the real and imaginary parts of the dielectric function of a hydrided Ho film are displayed for a few particular concentrations.

Congruent with the resistivity results, the overall evolution of the dielectric function of the Ho:H system is to a semi-

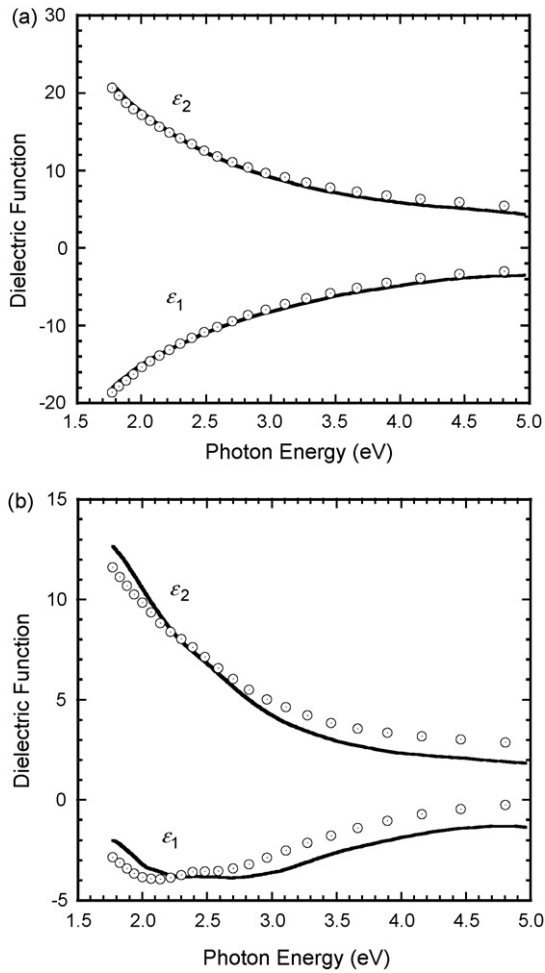


Fig. 3. Optimized values of the dielectric function: (a) of a Pd layer 12.6 nm thick and (b) of a Ho film 50.1 nm thick. They (solid lines) were obtained from the as deposited bilayer optical transmittance spectrum. The circles specify some of the values taken from the literature as initial estimation.

conducting material. The behavior of ϵ_2 indicates that the absorption of light decreases significantly in the visible range as the HoH_3 composition is approached. The residual value in ϵ_2 indicates that some absorption is still occurring in the trihydride phase which may be due to the presence of localized states in the interband region that allow some energy absorption. ϵ_1 becomes less negative in the visible wavelength range, with small variations in the near UV and with a crossover defining a plasma frequency, this gives a value of $\hbar\omega_p = 2.30$ eV for the dihydride and tends to a value of 2.87 eV at the higher concentrations reached. Fig. 5b displays the blue shift of the plasma frequency when the film is exposed to increasing hydrogen pressures, the value for the crystalline Ho was also included as calculated from the values reported by Weaver and Lynch [15] as indicated in Fig. 5a.

Of particular interest is the semiconducting behavior of the Ho film with the highest hydrogen concentration in which the trihydride phase has formed. In this case the absorption coefficient, $\alpha = 4\pi K/\lambda$, is calculated and the result is plotted as a function of energy (Tauc plot) [16]. Best fit is found if indirect allowed transitions are assumed. From this plot (see Fig. 6), the

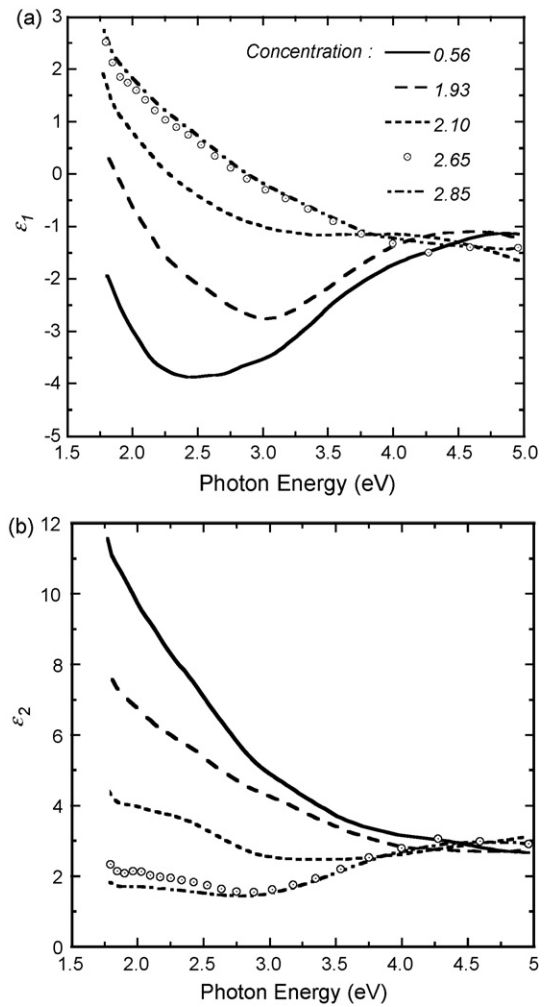


Fig. 4. Spectral dependence of the real (a) and imaginary (b) parts of the dielectric function of a hydrided Ho film 50.1 nm thick coated with a Pd layer of thickness 12.6 nm, for a few values of H concentration in the Ho film. Both parts of ϵ show the change towards the semi-conducting phase as hydrogen concentration increases.

optical gap has been estimated as $E_g = 3.30 \pm 0.05$ eV. This gap is compared with others found in the literature [17–19] for similar materials in Table 1. This table shows that Ho has the largest gap among the similar RE's trihydrides considered.

With the purpose of checking possible oxygen contamination during the hydrogenation process, one sample was submitted to

Table 1
Values of the optical band gaps for different trihydride rare earths; the first three are from our own calculations

Element	E_g (eV)
Ho	3.30
Tb	2.6
Dy	2.35
Gd	2.38 ^a ; 2.55 ^b
La	1.8 ^c
Y	2.4 ^c

^a From Ref. [17].

^b From Ref. [19].

^c From Ref. [18].

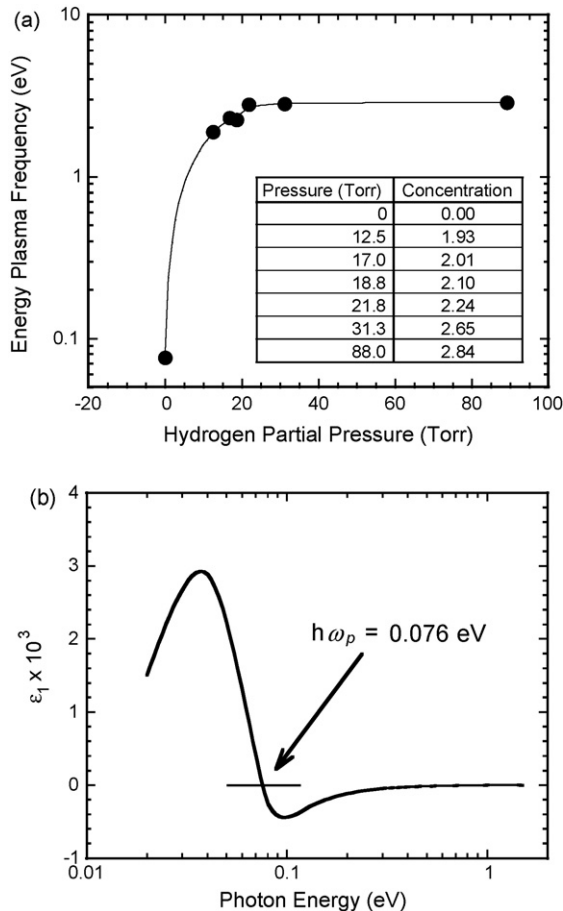


Fig. 5. (a) Energy plasma frequency of a hydrided Ho film under increasing hydrogen pressure, displaying the frequency shift from the IR to the near UV. The inset in Fig. 4a indicates the corresponding concentration values for each pressure. The value of $\hbar\omega_p$ for the crystalline Ho (non-hydrided) was calculated from the spectral behavior of ϵ_1 given in Ref. [15], which is depicted in (b).

several hydrogenation cycles [20], calculating E_g at the end of each one; also the absorption coefficient in the region described by the Urbach rule, for energies lower than the optical gap, was calculated after each cycle. Neither E_g or α showed an appreciable

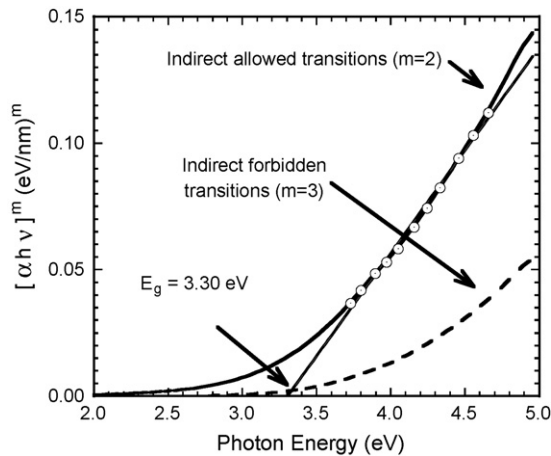


Fig. 6. Tauc plot to estimate the optical band gap from a Ho film 50.1 nm thick. Best fit is obtained assuming indirect allowed transitions ($m=2$) involved in the excitation of electrons through the gap characterizing the HoH₃ state.

change as a function of hydrogenation cycle. From the consistency of these parameters and the large difference between our estimated optical gap in HoH₃ phase and the holmium oxide gap: 5.2 eV [21], we conclude that the effect of oxidation is not significant in our samples.

4. Summary

The evolution of the electrical resistivity and the optical transmittance on hydrogenated Ho thin films shows a transition from the metallic state to the semi-conducting phase as hydrogen concentrations goes above 2.1. We have calculated the values of the dielectric function of films of Ho and its hydrided phases. For the semi-conducting trihydride phase we have also calculated a plasma frequency energy of 2.87 eV and a band gap of 3.30 eV.

Acknowledgements

The partial support from the Consejo Nacional para Investigaciones Científicas y Tecnológicas de Costa Rica (CONICIT) is gratefully acknowledged. Also the authors thank the valuable help of L.G. Loría who provided the quartz windows and substrates.

References

- [1] J.N. Huiberts, R. Griessen, J.H. Rector, R.J. Wijngaarden, J.P. Dekker, D.G. de Groot, N.J. Koeman, *Nature (London)* 380 (1996) 231.
- [2] K. von Rottkay, M. Rubin, F. Michalak, R. Armitage, T. Richardson, J. Slack, P.A. Duine, *Electrochim. Acta* 44 (1999) 3093.
- [3] I.A.M.E. Giebels, *Shining light on magnesium based switchable mirrors*, Ph.D. Thesis, Vrije Universiteit, Amsterdam, 2004.
- [4] R. Griessen, *Europhys. News* 32 (2001) 42.
- [5] K. Hirano, J. Kadono, S. Yamamoto, T. Tanabe, H. Miyake, *J. Alloy Compd.* 408–412 (2006) 351; P. Vajda, *Solid State Ionics* 168 (2004) 271.
- [6] J. Daou, P. Vajda, *Phys. Rev. B* 50 (1994) 12635; P. Vajda, in: K.A. Gschneidner Jr., L. Eyring (Eds.), *Handbook on the Physics and Chemistry of Rare Earths*, vol. 20, 1995, p. 207.
- [7] D. Azofeifa, N. Clark, W.E. Vargas, *Phys. Status Solidi (b)* 242 (2005) 2005.
- [8] D.E. Azofeifa, N. Clark, A. Amador, A. Saenz, *Thin Solid Films* 300 (1997) 295.
- [9] L.J. van der Pauw, *Res. Reports* 13 (1958) 1.
- [10] W.E. Vargas, D.E. Azofeifa, N. Clark, *Thin Solid Films* 425 (2003) 1.
- [11] A. Ramírez, W.E. Vargas, *Appl. Opt.* 43 (2004) 1508.
- [12] W.E. Vargas, I. Rojas, D.E. Azofeifa, N. Clark, *Thin Solid Films* 496 (2006) 189.
- [13] W.J. Tropf, M.E. Thomas, T.J. Harris, in: M. Bass (Ed.), *Handbook of Optics*, vol. II, McGraw Hill, New York, 1995, Chapter 33.
- [14] B.T. Sullivan, *Appl. Opt.* 29 (1990) 1964.
- [15] J.H. Weaver, D.W. Lynch, *Phys. Rev. Lett.* 34 (1975) 324.
- [16] J. Tauc, *Amorphous and Liquid Semiconductors*, Plenum, London, 1974.
- [17] E. Shalaan, H. Schmitt, K.H. Ehses, *Thin Solid Films* 489 (2005) 330.
- [18] A.T.M. van Gogh, D.G. Negengast, E.S. Kooij, N.J. Koeman, J.H. Rector, R. Griessen, *Phys. Rev. B* 63 (1999) 195105.
- [19] M.W. Lee, C.H. Lin, *J. Appl. Phys.* 87 (2000) 7798.
- [20] A. Miniotos, B. Hjörvarsson, L. Douysset, *Appl. Phys. Lett.* 76 (2000) 2056.
- [21] T. Wiktorczyk, *Thin Solid Films* 405 (2002) 238.